Distinctive local binary pattern for non-rigid registration of lung computed tomography images

Zhulou Cao and Enqing Dong[✉]

Non-rigid registration of lung computed tomography (CT) images is a valuable tool for various clinical applications. Many methods such as bilateral filters and census transform have been used to deal with discontinuity of lung motion and local intensity variation. However, census transform cannot distinguish between low and high contrast regions, which may lead to negative influence to differential-based registration methods. A novel distinctive local binary pattern that can generate distinctive representations of high contrast images is proposed. Combing the novel local binary pattern, bilateral filters, the inverse-consistent symmetrical method and the Lucas–Kanade method, a novel accurate image registration method is developed. The experiments are performed on the publicly available 4D CT lung dataset from DIR-Lab. Compared with the census transform, the proposed distinctive local binary pattern can achieve relatively better results. The proposed image registration method greatly improves the accuracy of the classical Lucas–Kanade method and the bilateral filters-based Demons. In addition, the proposed registration method is most accurate among all unmasked methods tested on this dataset.

Introduction: The task of medical image registration [1] is to find the correct spatial correspondences between two images. This task for lung computed tomography (CT) images is very challenging owing to dealing with discontinuity of motion and local intensity variations. Nevertheless, non-rigid registration of lung CT images has been proven to be an invaluable tool in many clinical applications such as image-guided radiation therapy and estimation of lung ventilation. Therefore, a lot of attention has been paid to non-rigid registration of lung CT images to improve registration accuracy in recent years.

Lung CT images often have high contrast regions. This can be seen from Fig. 1*b*, which plots the surface of the intensities of the entire CT image in Fig. 1*a*. Recently, census transform-based methods [2, 3] have been introduced to align lung CT images. Census transform generates binary vectors of all intensity differences between each pixel and its neighbourhood. In this way, census transform yields invariant representations to local intensity variation. However, this also enhances the image noise and decreases the contrast of the original CT image as shown in Fig. 1*c*. To obtain distinctive representations of images, we propose a novel local binary pattern named distinctive local binary pattern (DLBP). The proposed DLBP can generate distinctive representations of lung CT images as shown in Fig. 1*d*.

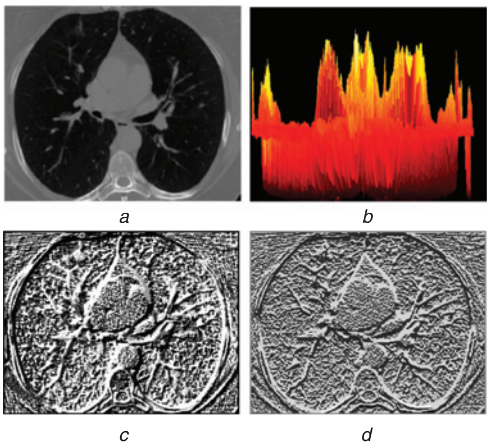

Fig. 1 *Comparison of DLBP and census transform*

a Original CT image
b Surface of intensities of original CT image
c Census transform of original CT image
d DLBP of original CT image

Bilateral filters-based Demons [4, 5] can cope well with discontinuity of lung motion. However, this method suffers from the low accuracy of registration. This Letter proposes a new accurate registration method that combines bilateral filters, the proposed DLBP, and the inverse-consistent symmetrical method, and Lucas–Kanade method.

Proposed DLBP: Let $\boldsymbol{I}$ denote an image, $\boldsymbol{I}(\boldsymbol{x})$ be the intensity at a point $\boldsymbol{x}$. Let $N_{\boldsymbol{x}}$ represents the neighbourhood of $\boldsymbol{x}$. DLBP consists of two binary vectors. The first binary vector is defined as

$$\boldsymbol{L}_1(\boldsymbol{x}) = \{g(\tau - \boldsymbol{I}(\boldsymbol{x}_1)), \ \ldots, g(\tau - \boldsymbol{I}(\boldsymbol{x}_p))\}, \tag{1}$$

where τ is the median of $\{\boldsymbol{I}(\boldsymbol{x}), \boldsymbol{I}(\boldsymbol{x}_1), \ldots, \boldsymbol{I}(\boldsymbol{x}_p)\}$, $\boldsymbol{x}_i \in N_{\boldsymbol{x}}$, $i = 1, \ldots, p$, and function $g(z)$ is defined as

$$g(z) = \begin{cases} 1 & \text{if} \quad z \geq 0 \\ 0 & \text{if} \quad z < 0 \end{cases}.$$

The second binary vector is expressed as

$$\boldsymbol{L}_2(\boldsymbol{x}) = \{f(\boldsymbol{I}(\boldsymbol{x}_1) - \boldsymbol{I}(\boldsymbol{x}'_1)), \ \ldots, f(\boldsymbol{I}(\boldsymbol{x}_m) - \boldsymbol{I}(\boldsymbol{x}'_m))\}, \tag{2}$$

where $\boldsymbol{x}_i \in N_{\boldsymbol{x}}$, $\boldsymbol{x}'_i \in N_{\boldsymbol{x}}$, $i = 1, \ldots, m$, $\boldsymbol{x}_i$ and $\boldsymbol{x}'_i$ are symmetrical with respect to the centre point, and function f is defined as

$$f(z) = \begin{cases} 6 = (110)_2 & \text{if} \quad z \geq T_3 \\ 5 = (101)_2 & \text{if} \quad z \geq T_2 \ \text{and} \ z < T_3 \\ 4 = (100)_2 & \text{if} \quad z \geq T_1 \ \text{and} \ z < T_2 \\ 3 = (011)_2 & \text{if} \quad z \geq -T_1 \ \text{and} \ z < T_1 \\ 2 = (010)_2 & \text{if} \quad z \geq -T_2 \ \text{and} \ z < -T_1 \\ 1 = (001)_2 & \text{if} \quad z \geq -T_3 \ \text{and} \ z < -T_2 \\ 0 = (000)_2 & \text{if} \quad z < -T_3 \end{cases},$$

where T_1, T_2, and T_3 are thresholds, and $0 < T_1 < T_2 < T_3$. Combining (1) and (2), we can obtain the DLBP as

$$\boldsymbol{L}(\boldsymbol{x}) = \{\boldsymbol{L}_1(\boldsymbol{x}), \ \boldsymbol{L}_2(\boldsymbol{x})\} \tag{3}$$

Proposed image registration method: The proposed image registration method consists of Lucas–Kanade method, the proposed DLBP, bilateral filters, and the inverse-consistent symmetrical method. We will discuss these four components sequentially in a 2D space for the sake of simplicity, although all the experiments of the proposed method will be performed in a 3D space.

First, we review Lucas–Kanade method. Let us assume that intensities of objects in subsequent frames are constant over time

$$\boldsymbol{I}(x + u, y + v, t + 1) = \boldsymbol{I}(x, y, t),$$

where $\boldsymbol{I}(x, y, t)$ is the intensity of pixel $\boldsymbol{x} = (x, y)$ in the frame t, and (u, v) is the displacement of the pixel between consecutive frames t and $t + 1$. For small displacements, we can perform a first-order Taylor expansion yielding

$$\boldsymbol{I}_x u + \boldsymbol{I}_y v + \boldsymbol{I}_t = 0, \tag{4}$$

where the subscripts denote partial derivatives. If the displacement is constant within some neighbourhood, the underdetermined (4) can be solved using weighted least square method by minimising the following objective:

$$E(u, v) = G_{lk} * \left((\boldsymbol{I}_x u + \boldsymbol{I}_y v + \boldsymbol{I}_t)^2\right),$$

where G_{lk} is the Gaussian filter. Then (u, v) can be obtained by the following linear system:

$$\begin{pmatrix} G_{lk} * (\boldsymbol{I}_x^2) & G_{lk} * (\boldsymbol{I}_x \boldsymbol{I}_y) \\ G_{lk} * (\boldsymbol{I}_x \boldsymbol{I}_y) & G_{lk} * (\boldsymbol{I}_y^2) \end{pmatrix} \begin{pmatrix} u \\ v \end{pmatrix} = -\begin{pmatrix} G_{lk} * (\boldsymbol{I}_x \boldsymbol{I}_t) \\ G_{lk} * (\boldsymbol{I}_y \boldsymbol{I}_t) \end{pmatrix} \tag{5}$$

Let $\boldsymbol{I}_1$ and $\boldsymbol{I}_2$ denote the target image and source image, respectively. The proposed method estimates forward transform (u_1, v_1) and backward transform (u_2, v_2) at the same time.

Then, we compute the DLBP of $\boldsymbol{I}_1$ and $\boldsymbol{I}_2$ using $\boldsymbol{I}_i^l(x, y) = \boldsymbol{L}(\boldsymbol{I}_i(x, y))$, $i = 1, 2$, where $\boldsymbol{L}(\cdot)$ denotes the DLBP defined in (3). We differentiate DLBP from the original image by an extra superscript l.

Next, we calculate the following gradients for the forward transform

$$\begin{cases} \boldsymbol{I}_x(x, y) = ||\boldsymbol{I}_2^l(x + 1, y) - \boldsymbol{I}_1^l(x, y)||_1 - ||\boldsymbol{I}_2^l(x - 1, y) - \boldsymbol{I}_1^l(x, y)||_1 \\ \boldsymbol{I}_y(x, y) = ||\boldsymbol{I}_2^l(x, y + 1) - \boldsymbol{I}_1^l(x, y)||_1 - ||\boldsymbol{I}_2^l(x, y - 1) - \boldsymbol{I}_1^l(x, y)||_1 \\ \boldsymbol{I}_t(x, y) = ||\boldsymbol{I}_2^l(x, y) - \boldsymbol{I}_1^l(x, y)||_1 \end{cases},$$

where l_1-norm for a vector $\boldsymbol{d} = (d_1, d_2, \ldots, d_n)$ is defined as $||\boldsymbol{d}||_1 = \sum_{i=1}^{n} |d_i|$. With these gradients, we compute forward transform (u_1, v_1) by solving the linear system (5). Similarly, we compute backward transform (u_2, v_2) with the following gradients:

$$\begin{cases} \boldsymbol{I}_x(x, y) = ||\boldsymbol{I}_1^l(x+1, y) - \boldsymbol{I}_2^l(x, y)||_1 - ||\boldsymbol{I}_1^l(x-1, y) - \boldsymbol{I}_2^l(x, y)||_1 \\ \boldsymbol{I}_y(x, y) = ||\boldsymbol{I}_1^l(x, y+1) - \boldsymbol{I}_2^l(x, y)||_1 - ||\boldsymbol{I}_1^l(x, y-1) - \boldsymbol{I}_2^l(x, y)||_1 \\ \boldsymbol{I}_t(x, y) = ||\boldsymbol{I}_1^l(x, y) - \boldsymbol{I}_2^l(x, y)||_1 \end{cases}$$

After that, we regularise (u_1, v_1) and (u_2, v_2) by the following bilateral filter [5]:

$$\boldsymbol{u}_{\text{new}}(\boldsymbol{x}) = \frac{1}{w(\boldsymbol{x})} \sum_{\boldsymbol{x}' \in N_x} G_x(\boldsymbol{x}, \boldsymbol{x}') G_I(\boldsymbol{I}(\boldsymbol{x}), \boldsymbol{I}(\boldsymbol{x}')) \\ G_u(\boldsymbol{u}(\boldsymbol{x}), \boldsymbol{u}(\boldsymbol{x}'))\boldsymbol{u}(\boldsymbol{x}')$$

where G_x, G_I, and G_u are Gaussian functions of distances, intensities and deform fields, respectively, $w(\boldsymbol{x})$ is a normalisation factor for the neighbourhood $\boldsymbol{N}_x$, and $\boldsymbol{u} = (u_1, v_1)$ or $\boldsymbol{u} = (u_2, v_2)$.

Finally, we apply the inverse-consistent symmetric method [6] to generate a new forward transform $(u'_1, v'_1)$and a new backward transform (u'_2, v'_2) by the following equations:

$$\begin{cases} (u'_1, v'_1) = (0.5u_1, 0.5v_1)o(0.5u_2^{-1}, 0.5v_2^{-1}) \\ (u'_2, v'_2) = (0.5u_2, 0.5v_2)o(0.5u_1^{-1}, 0.5v_1^{-1})' \end{cases}$$

where the notation o denotes the composition of two transforms.

In summary, each iteration of the proposed method consists of calculation of DLBP, forward and backward transformation estimation, bilateral filtering and inverse-consistent symmetric method.

Experimental results: All the optimal parameters are based on our experimental results. The proposed method adopts a coarse-to-fine strategy which consists of four levels with iterations {3, 3, 3, 2}, respectively. The window size is initialise with 11, which increases 2 at each level of image pyramids. The standard deviations of the Gaussian filters G_{Ik}, G_x, G_I, and G_u are {11/6, 310, 13/6, 5}, respectively.

The thresholds for DLBP are {2, 10, 800} for T_1, T_2, and T_3, respectively. We calculate partial points in a $5 \times 5 \times 5$ neighbourhood for DLBP. Let $\boldsymbol{\omega}_1 = \{(0, 0, 1), (0, 1, 0), (1, 0, 0)\}$ and $\boldsymbol{\omega}_2 = \{(1, 1, 1), (1, 1, -1), (1, -1, 1), (1, -1, -1), -\boldsymbol{\omega}_i = \{-\boldsymbol{x}|\boldsymbol{x} \in \boldsymbol{\omega}_i\}, i = 1, 2,$ and $2\boldsymbol{\omega}_1 = \{2\boldsymbol{x}|\boldsymbol{x} \in \boldsymbol{\omega}_1\}$. Given a point $\boldsymbol{x}$, then the set of selected points is $\boldsymbol{N_x} = \{\boldsymbol{x} + \boldsymbol{a}|\boldsymbol{a} \in \{\boldsymbol{\omega}_1 \cup (-\boldsymbol{\omega}_1) \cup \boldsymbol{\omega}_2 \cup (-\boldsymbol{\omega}_2) \cup (2\boldsymbol{\omega}_1)\}\}$. The DLBP of a 3D lung CT image is calculated using the above-mentioned parameters. One slice of the 3D CT lung and the corresponding slice of the DLBP are shown in Figs. 1*a* and *d*.

The experiments are tested on the publicly available 4D CT lung dataset from DIR-Lab [7]. We focus on the registration of the maximum inhalation and exhalation phase images. For each pair of images, 300 anatomical landmark pairs have been annotated. In all experiments, target registration error (TRE) for all landmarks is computed, which are the Euclidean distances between the landmark positions in the target image and the positions of the transformed reference landmarks.

Table 1: Mean and standard deviation of target registration errors (mm)

Case	Proposed	Lucas–Kanade	Census transform	Demons [5]
1	**0.85 ± 0.91**	1.05 ± 1.14	0.86 ± 0.93	1.05 ± 0.6
2	**0.82 ± 0.93**	1.09 ± 1.36	0.85 ± 0.95	1.08 ± 0.6
3	**0.94 + 1.05**	1.90 ± 2.03	0.95 ± 1.05	1.49 ± 0.9
4	**1.32 ± 1.28**	1.88 ± 1.81	1.39 ± 1.31	1.90 ± 1.3
5	**1.32 + 1.56**	2.61 ± 3.21	1.47 ± 1.78	1.99 ± 1.7
6	**1.15 ± 1.06**	4.42 ± 4.32	1.28 ± 1.26	2.36 ± 1.9
7	**1.27 + 1.37**	2.99 ± 2.79	1.62 ± 2.11	2.32 ± 1.9
8	**1.53 ± 2.11**	7.14 ± 6.82	2.12 ± 3.42	3.58 ± 3.4
9	**1.10 ± 1.00**	2.01 ± 1.77	1.22 ± 1.15	1.74 ± 1.0
10	**1.13 ± 1.36**	3.25 ± 3.92	1.27 ± 1.58	2.02 ± 2.1
Average	**1.14 ± 1.26**	2.83 ± 2.91	1.30 ± 1.55	1.95 ± 0.7

To evaluate our contributions, we implement the classical Lucas–Kanade. In addition, we replace DLBP and bilateral filters with census transform. Table 1 summarises the mean and standard deviation of TRE of these methods. Minimum values are highlighted with bold letters. For a comprehensive comparison, Table 1 includes the results of the bilateral filters-based Demons [5]. As shown in Table 1, the proposed method is far better than the classical Lukas–Kanade method. Compared with census transform, the combination of DLBP and bilateral filters can obtain results that are more accurate. Compared with existing bilateral filters-based Demons [5], our method can achieve accurate results with an improvement about 0.81 mm.

The proposed method achieves mean target registration error of 1.14 mm on the 4D CT dataset from DIR-Lab. To best of our knowledge, the top three results of mean target registration errors for unmasked registration for this dataset are 1.17 [8], 1.34 [2], and 1.41 mm [3]. Therefore, the proposed method is the accurate for unmasked registration tested on this dataset. This is only slightly higher than the best result of the masked registration 0.94 mm [9].

The proposed method is implemented using MATLAB on a computer with a 3.1 GHz Intel® Core i7 Quad-Core Processor. The runtime of the proposed method for a pair of $256 \times 256 \times 99$ images is about 15 min, which is 4 to 5 times faster than the bilateral filters-based Demons [5].

Conclusion: A novel local binary pattern and a novel non-rigid registration method are proposed. The proposed local binary pattern can generate more distinctive representations of lung CT images than census transform. The proposed registration method achieves a mean target registration error of 1.14 mm, which is most accurate of all unmasked registration methods tested on the 4D CT lung dataset from DIR-Lab.

Acknowledgments: This work was supported by the Natural Science Foundation of China (grants 81371635 and 11401346).

Submitted: *16 February 2015*
doi: 10.1049/el.2015.0598
One or more of the Figures in this Letter are available in colour online.

Zhulou Cao and Enqing Dong (*School of Mechanical, Electrical and Information Engineering, Shandong University (Weihai), 180 Wenhua Xilu, Weihai 264209, People's Republic of China*)

✉ E-mail: enqdong@sdu.edu.cn

References

1 Cao, Z.L., and Dong, E.Q.: 'Multi-modal image registration using edge neighbourhood descriptor', *Electron. Lett.*, 2014, **50**, (10), pp. 752–754, doi: 10.1049/el.2014.0795
2 Hermann, S., and Werner, R.: 'TV-L1-based 3D medical image registration with the census cost function', *Image Video Technol. Lect. Notes Comput. Sci.*, 2014, **8333**, pp. 149–161, doi: 10.1007/978-3-642-53842-1_13
3 Hermann, S., and Werner, R.: 'High accuracy optical flow for 3D medical image registration using the census cost function', *Image Video Technol. Lect. Notes Comput. Sci.*, 2014, **8333**, pp. 23–35, doi: 10.1007/978-3-642-53842-1_3
4 Thirion, J.P.: 'Image matching as a diffusion process: an analogy with Maxwell's demons', *Med. Image Anal.*, 1998, **2**, (3), pp. 243–260, doi: 10.1016/S1361-8415(98)80022-4
5 Papież, B.W., Heinrich, M., Fehrenbach, J., *et al.*: 'An implicit sliding-motion preserving regularisation via bilateral filtering for nonrigid image registration', *Med. Image Anal.*, 2014, **18**, (8), pp. 1299–1311, doi: 10.1016/j.media.2014.05.005
6 Heinrich, M., Jenkinson, M., Brady, M., *et al.*: 'MRF-based nonrigid registration and ventilation estimation of lung CT', *IEEE Trans. Med. Imaging*, 2013, **32**, (7), pp. 1239–1248, doi: 10.1109/TMI.2013.2246577
7 Castillo, R., Castillo, E., Guerra, R., *et al.*: 'A framework for evaluation of nonrigid image registration spatial accuracy using large landmark point sets', *Phys. Med. Biol.*, 2009, **54**, pp. 1849–1870, doi: 10.1088/0031-9155/54/7/001
8 Heinrich, M., Papiez, B., Schnabel, J., *et al.*: 'Non-parametric discrete registration with convex optimisation'. Int. Workshop on Biomedical Image Registration, London, UK, July 2014, pp. 51–61, doi: 10.1007/978-3-319-08554-8_6
9 König, L., and Rühaak, J.: 'A fast and accurate parallel algorithm for non-linear image registration using normalized gradient fields'. IEEE Int. Symp. on Biomedical Imaging, Beijing, China, April 2014, pp. 580–583, doi: 10.1109/ISBI.2014.6867937